

BASE OF TONGUE CANCER

CASE STUDY

QUYNH-THU LE, MD, TODD PAWLICKI, PHD

Patient History

A 52-year-old male presented with odynophagia and intermittent right-sided otalgia. On a complete head and neck evaluation, he was noted to have an exophytic right base of tongue (BOT) mass involving the glossotonsillar sulcus, pharyngoepiglottic fold, and vallecula. A head and neck magnetic resonance image (MRI) revealed a $3.8 \times 2.6 \times 2.7 \text{ cm}^3$ T₂-weighted hyperintense lesion involving the right BOT and the right lateral oropharyngeal wall (Figure 18.4-1). There were multiple enlarged right-sided cervical nodes. In addition, there was a small node ($< 10 \text{ mm}$ in short axis) in the left level II region. Panendoscopy and biopsy of the tumor revealed moderately differentiated invasive squamous cell carcinoma. A positron emission tomography (PET) scan that was performed for staging and treatment planning confirmed increased metabolic uptake in the right BOT and right-sided cervical nodes. In addition, it showed increased metabolic uptake in a left level II neck node (Figure 18.4-2A). The patient was therefore staged as having a T₂N₂CM₀ squamous cell carcinoma of the BOT and was recommended to receive concurrent chemoradiotherapy with the radiation delivered via an intensity-modulated radiation therapy (IMRT) approach.

Simulation

The patient was immobilized in an Aquaplastic mask (Aquaplast, Wycoff Heights, NJ). A custom-made head and neck immobilization device was used to maximize reproducibility of the head and chin position (Figure 18.4-3A; AccuForm, MED-TEC Inc., Orange City, IA). In addition, the shoulders were immobilized by having the patient hold on to two hand dowels or pegs on a customized plastic board. The location of the hand dowels can be adjusted for each patient to maximize the patient's comfort and reproducibility of the position. Figure 18.4-3B shows the patient in the treatment position. Simulation studies show that this device can immobilize the shoulders with 2 to 3 mm anterior-posterior (A-P) and left-right (L-R) maximal daily variability. The addition of an Aquaplastic shoulder immobilization system to this device does not improve the daily reproducibility and increases skin dose to the lower neck area.¹ In addition, three tattoos were placed over the shoulder and anterior chest wall to maximize daily setup reproducibility.

A computed tomography (CT) scan was obtained with the patient in the treatment position on the PQ 5000 CT scanner (Philips Medical Systems, Andover, MA). Routine

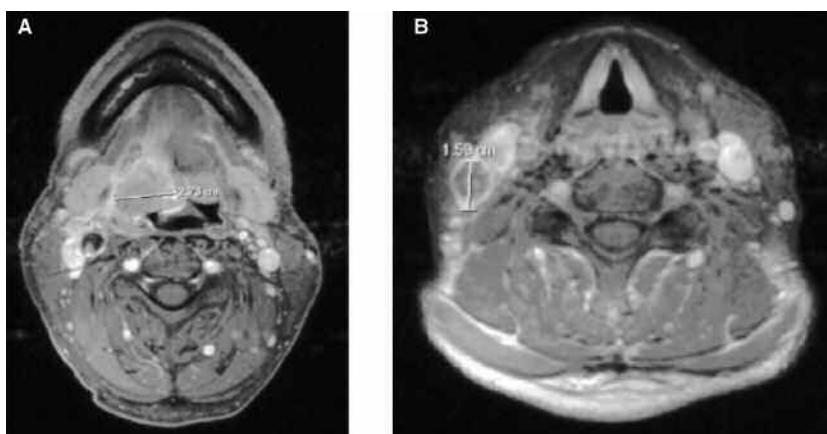


FIGURE 18.4-1. Axial images from pretreatment magnetic resonance imaging showing (A) a right tongue base cancer and (B) a necrotic right level III neck node.

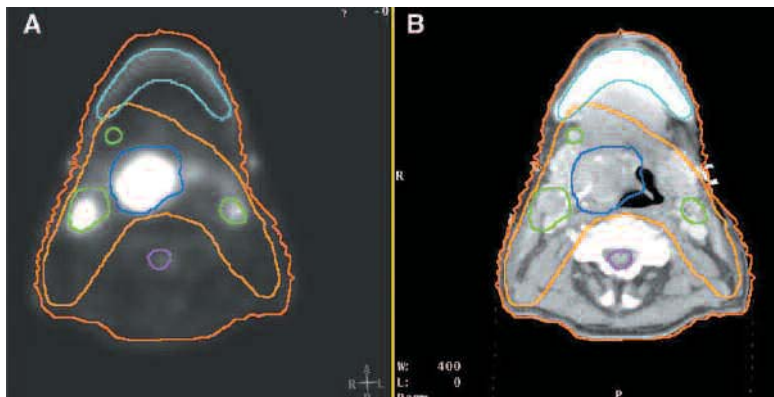


FIGURE 18.4-2. (A) Axial image of the staging positron emission tomography (PET) scan showing increased metabolic uptake in the right base of the tongue and right level II and left level II neck nodes. (B) Treatment planning computed tomography scan showing target and normal tissue contours of primary tumor gross tumor volume (*dark blue*), nodal gross tumor volume (*green*), planning target volume (*light orange*), mandible (*light blue*), skin (*dark orange*), and spinal cord (*purple*). (To view a color version of this image, please refer to the CD-ROM.)



FIGURE 18.4-3. (A) Picture of an AccuForm custom-made head and neck support. (B) Patient immobilized for treatment on an institutional custom-made shoulder immobilization device using hand dowels. (To view a color version of this image, please refer to the CD-ROM.)

administration of intravenous contrast (150 cc of Visipaque [Iodixanol] in a contrast injector) is used in most patients receiving head and neck IMRT who have adequate renal function and no history of contrast allergy. Axial CT slices of 3 mm thickness were obtained from the skull base to the carina. Figure 18.4-2B illustrates a cross-sectional image through the BOT on the treatment planning CT scan.

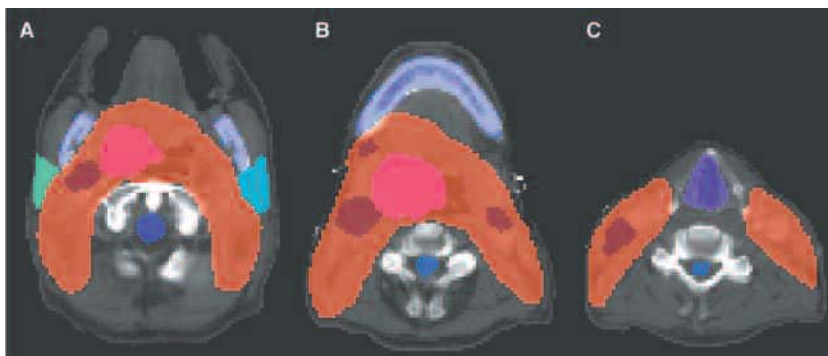
We are presently conducting a systematic study to determine the impact of ^{18}F -fluorodeoxyglucose (^{18}FDG) PET on radiation treatment planning in head and neck cancers. A fiducial-based system is used for the PET-CT fusion. As part of this protocol, three to five radiopaque fiducials are placed on the patient's mask and neck during the treatment planning CT scan. Patients then undergo a PET scan on a

GE Discovery LS PET/CT scanner (GE Healthcare, Waukesha, WI) in the same treatment planning position immobilized with the same mask and base-plate. For the PET fiducials, approximately $1\ \mu\text{Ci}$ of ^{18}FDG is mixed in $10\ \mu\text{L}$ of either water or normal saline. The PET scan is then fused to the appropriate treatment planning CT using the fiducial locations and the AcQSim VoxelQ fusion tools (Philips Medical Systems). For all of the patients in the study, the primary tumor is defined using the CT scan, whereas involved neck nodes are identified based on both CT pathologic nodal criteria (lymph nodes $\geq 1\ \text{cm}$ in short axis, spherically shaped small nodes in the draining lymphatic regions, nodes with radiographic evidence of necrosis or extracapsular extension and cluster of three or more borderline-sized nodes) and ^{18}FDG PET criteria (all lymph nodes with increased metabolic activity, regardless of nodal size).

Target and Tissue Delineation

We usually use contrast-enhanced CT and, whenever possible, MRI-CT fusion for delineation of the primary tumor. In this case, MRI was used complementary to the treatment planning CT for tumor definition, but fusion was not performed because the MRI was obtained at an outside institution. In our experience, both CT and MRI provide excellent anatomic details for BOT cancers, with the exception of patients with metallic dental fillings, in whom MRI

FIGURE 18.4-4. Representative cross-sectional images from the treatment planning computed tomography (CT) scan showing gross tumor volume contours of the primary tumor (*bright red*), involved neck nodes (*dark red*), planning target volume (*orange*), right parotid gland (*light green*), left parotid gland (*light blue*), mandible (*light violet*), true vocal cords (*purple*), brainstem (*dark purple*), and spinal cord (*dark blue*). (To view a color version of this image, please refer to the CD-ROM.)



is superior to CT. ^{18}F FDG PET, on the other hand, lacks the anatomic details for tumor definition and is not useful for defining primary tumors, except in situations of PET-CT hybrid scans or accurate PET-CT fusion. The opposite is true for nodal staging. Multiple studies have suggested that ^{18}F FDG PET is more sensitive and specific in evaluating nodal metastasis than CT or MRI.²⁻⁵ Emerging studies with hybrid PET-CT devices demonstrated that the fused image is superior to either image alone for the staging and management of solid tumors.^{6,7} Based on the above information, we recommend using the combination of PET and CT scans for contouring involved neck nodes in head and neck cancer patients based on the criteria described previously. Figure 18.4-4 shows target definition of the primary tumor and nodal gross tumor volumes (GTVs) for this case.

In this case, the clinical target volume (CTV) for the primary tumor included the entire BOT, vallecula, ipsilateral tonsillar bed, epiglottis, and preepiglottic space. A 1 to 3 cm anterior margin was also included. The CTV for the regional nodes included ipsilateral level 1b owing to anterior tumor extension and involvement of level II nodes, bilateral level II to V nodes, and upper mediastinal nodes owing to tumor involvement of the ipsilateral level IV region. In addition, the CTV and planning target volume (PTV) of the ipsilateral level II nodes were extended to the skull base to ensure

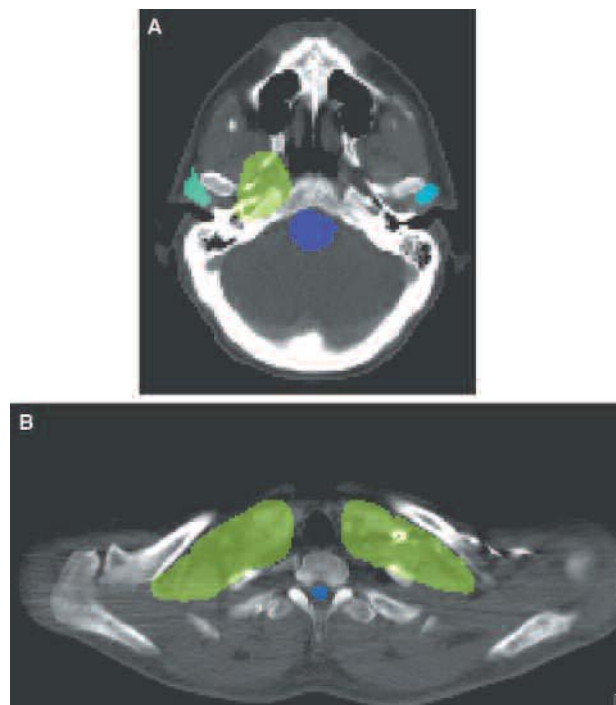


FIGURE 18.4-5. Representative cross-sectional images of the treatment planning computed tomography (CT) showing (A) planning target volume (PTV) extension into the skull base on the right side to ensure adequate coverage of the ipsilateral retropharyngeal lymph nodes and (B) PTV contours of the lower neck nodes. (To view a color version of this image, please refer to the CD-ROM.)

adequate coverage of the superior retropharyngeal nodes (Figure 18.4-5A). On occasions, excessive large hot spots are noted in certain areas of the neck after generating the initial IMRT plans owing to the extensive nodal coverage in the PTV (from the skull base to the carina). These areas can be contoured as separate nodal structures. This approach provides more control over the optimization and minimizes excessive dose to these locations (Figure 18.4-6 and the PTV2 dose-volume histogram [DVH] in Figure 18.4-10).

The following normal tissues are routinely outlined for BOT cancers: the eyes, optic nerves, optic chiasm, brainstem, individual parotid glands, mandible, glottic larynx, and spinal cord. In this case, owing to extensive nodal involvement, we elected to spare only the superficial parotid lobes and therefore did not include the deep lobes when outlining the parotid glands. On occasion, excessive hot or cold spots are noted in certain regions of the PTV after generating the initial IMRT plans. Specialized structures named “tuning structures” are added for the purpose of minimizing hot spots outside the target volume(s) and generating a conformal dose distribution for head and neck IMRT plans (Figure 18.4-7).

Treatment Planning

Typical values for head and neck immobilization and setup uncertainty are A-P 1.1 ± 2.3 mm, superior-inferior 0.9 ± 2.3 mm, and L-R 0.8 mm.⁸ These margins are included in our contours of the tumor and upper neck CTV to create the PTV used for treatment planning and dose evaluation. As previously mentioned, the interfraction organ setup uncertainty for our custom-made immobilization

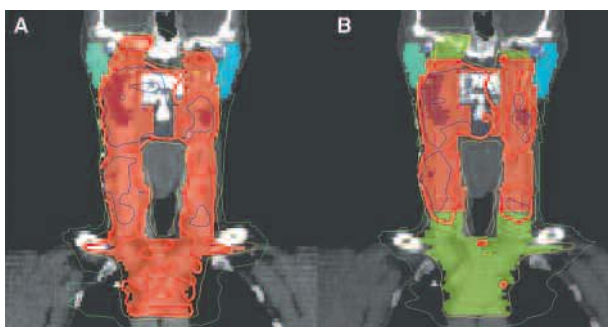


FIGURE 18.4-6. Coronal slice showing the importance of separating the planning target volume (PTV) into two parts to improve dose homogeneity. (A) The PTV contoured as one structure (red) with the 60 Gy isodose curve (red) extending superiorly into the skull base and inferiorly into the mediastinum. (B) The PTV divided into two separate structures (red and green) and a subsequent reduction in the 60 Gy isodose curve superiorly and inferiorly. Corresponding dose-volume histograms are shown in Figure 18.4-10. The isodose curves shown in this figure are 66 Gy (dark blue), 60 Gy (red), 54 Gy (yellow), and 40 Gy (green). The 60 Gy isodose curve is shown thicker to highlight the differences. (To view a color version of this image, please refer to the CD-ROM.)

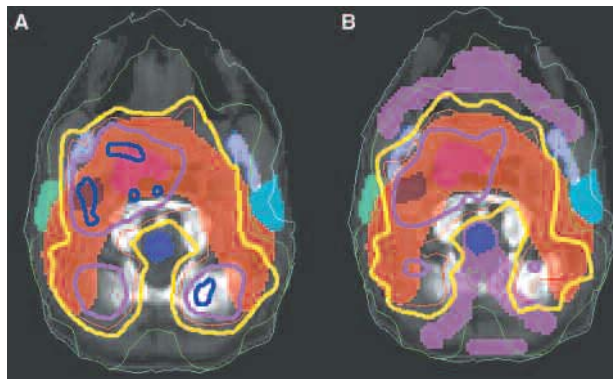


FIGURE 18.4-7. This figure shows the effect of a tuning structure in improving the dose distribution conformity. (A) The plan was optimized without a tuning structure, and (B) the plan was optimized with a tuning structure (light purple). The same dose constraints were used for both cases. The isodose curves shown in this figure are 73 Gy (dark blue), 66 Gy (purple), 60 Gy (red), 54 Gy (yellow), 40 Gy (green), and 20 Gy (light blue). Note the reduction in the left posterior 73 Gy hot spot in B while maintaining coverage of the base of tongue tumor and the involved lymph node. The 73 Gy, 66 Gy, and 54 Gy isodose curves are shown thicker to highlight the differences. (To view a color version of this image, please refer to the CD-ROM.)

device ranges from 2 to 3 mm. These margins are included in the PTV contours of the lower neck and upper mediastinum for treatment planning.

The prescription dose is 66 Gy in 30 fractions (2.2 Gy/fraction) to the GTV and 54 Gy in 30 fractions to the PTV (1.8 Gy/fraction). The planning parameters necessary to achieve this prescription are specific to the implementation of each optimization algorithm. The *CORVUS* inverse planning software version 4.0 (North American Scientific, NOMOS

Radiation Oncology Division, Cranberry Township, PA) was used to generate the IMRT plan for patient treatment. This software version uses a stochastic optimization algorithm with a pencil beam dose calculation algorithm. The IMRT treatment plans were calculated with heterogeneity correction turned on during both beamlet optimization and final dose calculation. The exact planning parameters used for this case are given in Table 18.4-1.

As previously mentioned in the target contouring section, a special arrangement of structures or tissue contours was used to produce the optimal dose distribution. Owing to the large volume of the PTV in this case (to treat all nodal regions from the skull base to the upper mediastinum), it is difficult to control the larger areas of hot spots throughout the PTV, as shown in the superior and inferior aspects of the PTV in Figure 18.4-6A. Figure 18.4-6B shows a coronal image of the contours where the PTV was split into two structures (PTV1 in orange and PTV2 in green). By breaking up the PTV volume, a more homogeneous dose coverage of the PTV is obtained. A tuning structure was placed adjacent to the target in noncontoured regions of the CT scan. The doses in Figure 18.4-7B were generated with the same optimization parameters as those in Figure 18.4-7A except that the tuning structure was added and used in the optimization procedure for Figure 18.4-7B. The use of tuning structures has proved to be an efficient method to obtain conformal dose distributions in head and neck IMRT planning using *CORVUS*.

It should be reiterated that the planning parameters shown here are specific to the *CORVUS* version 4.0 inverse planning system. Furthermore, they do not necessarily represent what is clinically required for the patient's treatment. They do, however, give the optimal isodose distribution and DVHs for treatment. The AcQSim segmentation tools

TABLE 18.4-1. Input Parameters

Structure Name	Goal/Limit, Gy	Volume below		Minimum, Gy	Maximum, Gy	Tissue Type
		Goal/above Limit, %	Limit, %			
GTV	66	2		65	68	Homogeneous
Node	66	2		65	68	Homogeneous
PTV1	54	5		53	56	Homogeneous
PTV2	52	5		50	54	Homogeneous
Nontarget tissue	45	0		0	45	Homogeneous
Spinal cord	30	5		30	40	Basic structure
Mandible	40	30		20	50	Basic structure
Brainstem	45	2		40	50	Basic structure
Larynx	25	30		11	45	Basic structure
RT parotid gland	30	10		25	60	Basic structure
LT parotid gland	20	2		15	50	Basic structure
Eyes	45	5		40	50	Basic structure
Optic nerves	45	5		40	50	Basic structure
Chiasm	45	5		40	50	Basic structure
Tuning structure	40	10		35	45	Basic structure

GTV = gross tumor volume; PTV = planning target volume.

were used for tumor and normal tissue contouring. The AcQSim system has a 16-structure limit on the number of structures permitted for each patient. Hence, for this case, it was required to combine the right and left eyes and the right and left optic nerves into one structure. This did not play a significant role in the optimization process because those structures are superior to the target volume.

The patient was treated on a Varian 2100EX (Varian Medical Systems, Palo Alto, CA) dual-energy linear accelerator. The plan was created with a 6 MV photon beam and $1 \times 1 \text{ cm}^2$ beamlets. On Varian accelerators, the maximum treatable field width in one beam-on time for IMRT is limited to 14.5 cm. This is due to the finite length of the Varian multileaf collimator leaves in the travel direction and the inability of collimator jaws to move during treatment. The CORVUS inverse planning system automatically accounts for these limitations by splitting a field into two fields if the target width exceeds the Varian field size limit in the beam's eye view. Therefore, although the treatment plan was developed with seven axial coplanar fields, the actual number of treated fixed fields was 15. The beam angles, in Varian convention, were 0 posterior-anterior (PA), 80 left posterior oblique (LPO), 120 left anterior oblique (LAO), 160 (LAO),

200 right anterior oblique (RAO), 240 (RAO), and 280 right posterior oblique (RPO) degrees.

The dose statistics for this treatment are summarized in Table 18.4-2. Isodose curves showing GTV coverage are shown in Figure 18.4-8. The maximum dose anywhere in the patient is 75.9 Gy and is located in the tumor volume. Only 1 cc of the target volume receives doses 74.0 Gy or greater. The maximum dose is located in the nodal region designated as PTV1 about 3 mm superior to the CT slice shown in Figure 18.4-8B. For nontarget tissue, only 1 cc receives doses 70.2 Gy or greater. The DVH shows that 97.7% of the GTV receives doses ≥ 66 Gy and 3.9% of the GTV receives doses > 72.6 Gy ($\geq 110\%$ of the prescription dose; Figure 18.4-10). The mean dose to the GTV was 69.4 Gy, whereas 97.2% of the involved neck nodes receives doses ≥ 66 Gy and 2.8% receives doses > 72.6 Gy.

PTV2 was defined as the nodal regions superior and inferior to the region of the tumor and the involved neck nodes. The isodose curves for PTV2 are shown in Figure 18.4-9. The dose homogeneity is particularly good in these regions. The DVHs show that 94.5% of PTV2 receives 54 Gy (prescription dose) and 6.1% receives doses > 59.4 ($> 110\%$ of the prescription dose; Figure 18.4-10). Within

TABLE 18.4-2. Dose Statistics

Structure Name	Goal/Limit, Gy	Volume below Goal/above Limit, %	Minimum, Gy	Maximum, Gy	Mean, Gy
GTV	66.0	2.2	64.1	75.5	69.4
Node	66.0	2.7	63.3	74.0	69.5
PTV1	54.0	4.3	30.3	75.9	61.5
PTV2	54.0	2.7	40.6	67.1	56.4
Nontarget tissue	45.0	7.7	0.0	72.1	13.4
Spinal cord	30.0	28.8	12.5	44.4	29.1
Mandible	40.0	71.4	14.8	69.0	45.0
Brainstem	45.0	4.4	5.7	49.7	24.8
Larynx	25.0	41.9	18.2	42.9	25.3
RT parotid gland	30.0	39.9	14.8	63.0	30.4
LT parotid gland	20.0	53.0	11.4	50.5	21.8
Eyes	45.0	0.0	1.9	3.0	2.3
Optic nerves	45.0	0.0	2.3	3.0	2.6
Chiasm	45.0	0.0	3.0	4.2	3.3

GTV = gross tumor volume; PTV = planning target volume. Maximum, minimum, and mean values reflect the final plan approved for treatment.

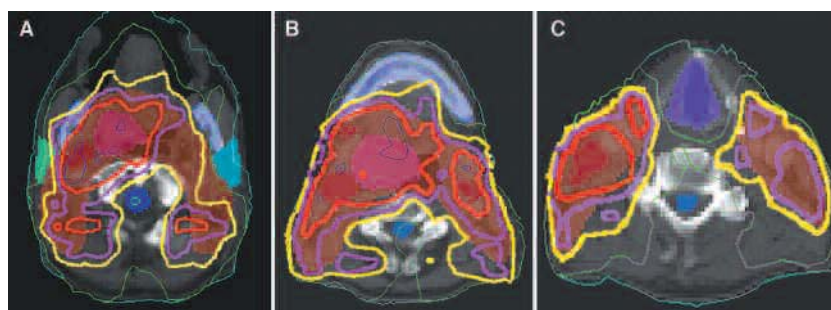


FIGURE 18.4-8. Isodose curves illustrating coverage of the gross tumor volume (GTV) and planning target volume (PTV). The isodose curves shown in this figure are 73 Gy (dark blue), 66 Gy (red), 60 Gy (purple), 54 Gy (yellow), 40 Gy (green), and 20 Gy (light blue). The prescribed doses are 66 Gy at 2.2 Gy/fraction to the GTV and 54 Gy at 1.8 Gy/fraction to the PTV. (To view a color version of this image, please refer to the CD-ROM.)

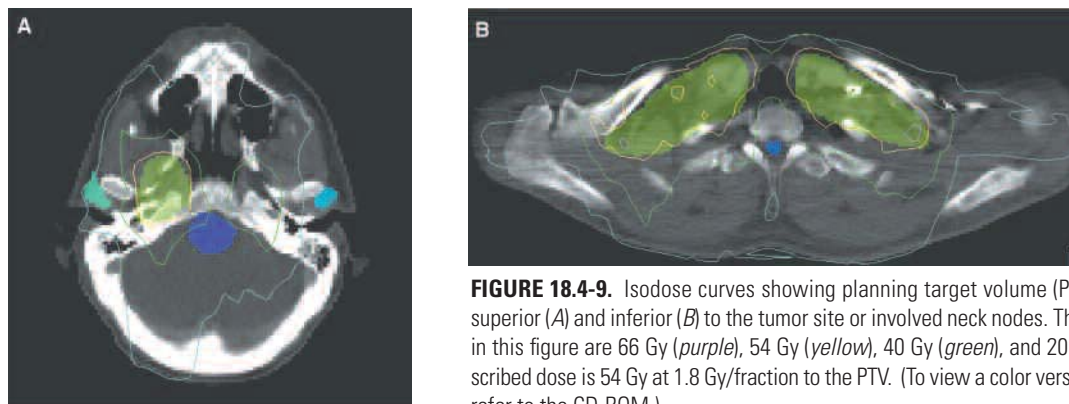


FIGURE 18.4-9. Isodose curves showing planning target volume (PTV) coverage in regions superior (A) and inferior (B) to the tumor site or involved neck nodes. The isodose curves shown in this figure are 66 Gy (purple), 54 Gy (yellow), 40 Gy (green), and 20 Gy (light blue). The prescribed dose is 54 Gy at 1.8 Gy/fraction to the PTV. (To view a color version of this image, please refer to the CD-ROM.)

the PTV1 that surrounds the BOT tumor and involved neck nodes, 95.7% receives doses ≥ 54 Gy, whereas 63.2% receives doses $\geq 110\%$ of the prescription dose. The large volume of PTV1 receiving high doses is expected because all of the GTVs are located within this volume by definition.

The maximum brainstem dose is 49.7 Gy, whereas ≤ 1 cc of the brainstem volume receives ≥ 45.6 Gy. For the spinal cord, the maximum dose is 44.4 Gy and ≤ 1 cc of the contoured volume receives ≥ 40.0 Gy. The mean doses to the larynx, right parotid gland, and left parotid gland are 25.3, 30.4, and 21.8 Gy, respectively. The optic apparatus is located far from the treated regions, and the maximum dose to any of these structures is 4.2 Gy over 30 fractions. The DVHs for all structures are shown in Figures 18.4-10 and 18.4-11.

Treatment Delivery and Quality Assurance

Before starting treatment, all patients receiving head and neck IMRT at Stanford University undergo a verification

step, during which the immobilization system is checked, the orthogonal images of the isocenter(s) are reproduced on simulation films for better visualization of bony landmarks, and the lower neck fields are defined in cases in which the lower neck is treated with conventional techniques. In this patient, the primary tumor and the entire neck were comprehensively treated with IMRT; therefore, only the IMRT isocenter location was verified. Figure 18.4-12A shows the A-P digitally reconstructed radiograph and Figure 18.4-12B shows a lateral digitally computed radiograph (DCR) of the isocenter. The DCR uses additional manipulation of the CT data to enhance the bony anatomy for better comparison with either simulation or portal films. Also note that the lateral DCR shown in Figure 18.4-12B is created using half of the patient's CT data. The image gives the impression of looking inside the cranium. This technique is useful for enhancing the skull base, sella turcica, and cervical spine processes. The simulation and portal images of the isocenter are shown in Figure 18.4-12C–F. During the active treatment period, portal images

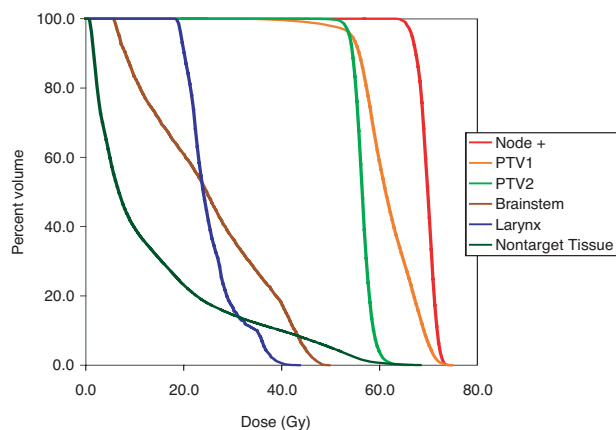


FIGURE 18.4-10. Dose-volume histograms of the involved neck nodes (Node+), planning target volumes (PTV), and selected normal tissues.

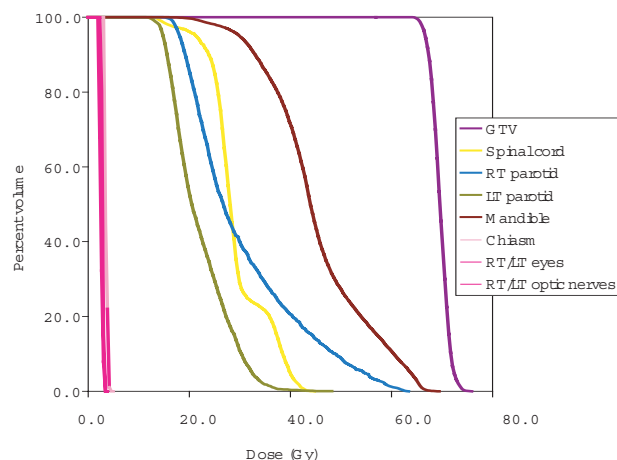


FIGURE 18.4-11. Dose-volume histograms of a primary tumor (gross tumor volume [GTV]) and selected normal tissues.

of the isocenter and the lower neck fields are taken weekly or more often if necessary. In addition, outlines of the modulated anatomic region for each beam angle are filmed at the beginning of treatment to ensure the accuracy of the isocenter location.

At our institution, all IMRT treatments are delivered using the step and shoot technique. For the 7 beam angles

(and 15 total beams), approximately 18.8 minutes of beam-on time is necessary to deliver 1,763 monitor units in this case. The overall duration for each treatment session, which includes both beam-on time and patient setup, is approximately 37 minutes. Acquisition of weekly isocenter portal films typically adds 3 to 5 minutes to the entire process 1 day a week. For a conventional five-field head and neck treatment (L-R lateral opposed photon fields, L-R posterior neck electron fields, and an A-P supraclavicular field), approximately 22 minutes is required for each treatment session. Overall, the IMRT treatment time is about 15 minutes longer than conventional head and neck treatment for each session. Inverse planning systems that provide more control over field splitting should allow IMRT treatment plans to be developed with fewer beams, yet are dosimetrically comparable to the plan described here. In this case, IMRT treatment times should be comparable to conventional treatment times.

Clinical Outcome

The patient completed the radiation treatment course in 6 weeks without any interruption. He also received two cycles of cisplatin and 5-fluorouracil concurrently with radiotherapy. He did not receive the third course of chemotherapy owing to grade 4 granulocytopenia. His treatment course was complicated by protracted nausea and vomiting secondary to chemotherapy and thick mucus production, requiring frequent intravenous fluid hydration and placement of a percutaneous gastrostomy feeding tube. He lost a total of 16 lb (9.5% body weight) during active therapy. His feeding tube was removed 2 months after treatment, and a follow-up MRI at 3 months showed complete resolution of the BOT mass and bilateral neck node (Figure 18.4-13). The patient returned to work full time at approximately 1 month after completion of therapy and was disease free at 6 months with minimal (grade 1) xerostomia.

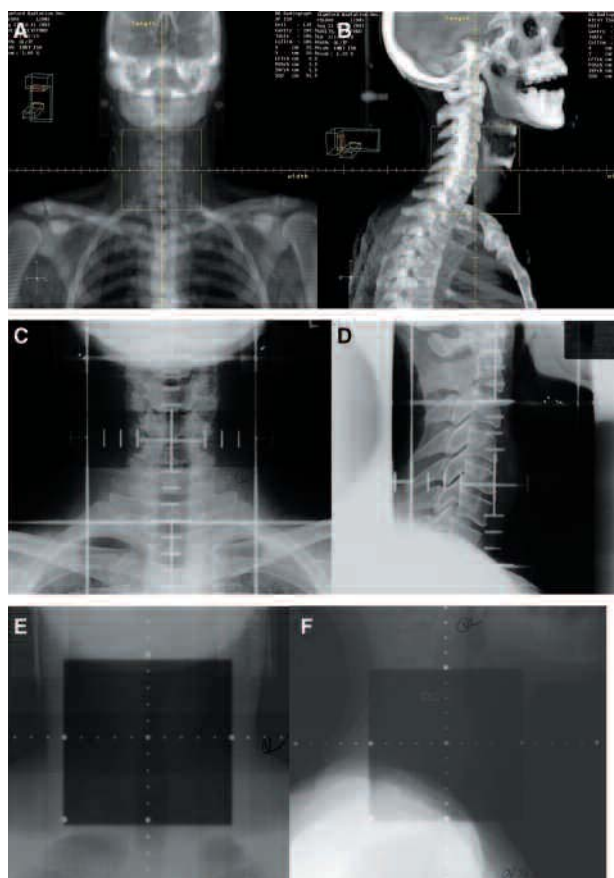


FIGURE 18.4-12. (A) Anterior-posterior (A-P) digitally reconstructed radiograph. (B) Lateral digitally computed radiograph. (C) A-P simulation film. (D) Lateral simulation film. (E) A-P portal image. (F) Lateral portal image.

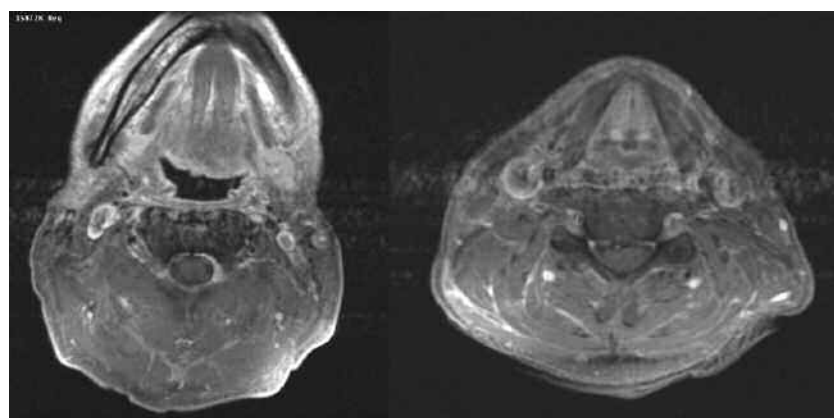


FIGURE 18.4-13. Axial images from follow-up magnetic resonance imaging at 3 months postradiation therapy. Note the complete resolution of the base of the tongue mass and bilateral neck node (see Figure 18.4-1).

References

1. Lee N, Chuang C, Quivey JM, et al. Skin toxicity due to intensity-modulated radiotherapy for head-and-neck carcinoma. *Int J Radiat Oncol Biol Phys* 2002;53:630–7.
2. Adams S, Baum RP, Stuckensen T, et al. Prospective comparison of 18F-FDG PET with conventional imaging modalities (CT, MRI, US) in lymph node staging of head and neck cancer. *Eur J Nucl Med* 1998;25:1255–60.
3. Stuckensen T, Kovacs AF, Adams S, et al. Staging of the neck in patients with oral cavity squamous cell carcinomas: a prospective comparison of PET, ultrasound, CT and MRI. *J Craniomaxillofac Surg* 2000;28:319–24.
4. Kao CH, Hsieh JF, Tsai SC, et al. Comparison of 18-fluoro-2-deoxyglucose positron emission tomography and computed tomography in detection of cervical lymph node metastases of nasopharyngeal carcinoma. *Ann Otol Rhinol Laryngol* 2000;109:1130–4.
5. Kau RJ, Alexiou C, Laubenbacher C, et al. Lymph node detection of head and neck squamous cell carcinomas by positron emission tomography with fluorodeoxyglucose F 18 in a routine clinical setting. *Arch Otolaryngol Head Neck Surg* 1999;125:1322–8.
6. Lardinois D, Weder W, Hany TF, et al. Staging of non-small-cell lung cancer with integrated positron-emission tomography and computed tomography. *N Engl J Med* 2003;348:2500–7.
7. Hany TF, Steinert HC, Goerres GW, et al. PET diagnostic accuracy: improvement with in-line PET-CT system: initial results. *Radiology* 2002;225:575–81.
8. Booth JT, Zavgorodni SF. Set-up error and organ motion uncertainty: a review. *Australas Phys Eng Sci Med* 1999;22:29–47.